JOURNAL OF BUILDING PHYSICS

*Article*

*Journal of Building Physics*
1–20

DOI: 10.1177/1744259115589680
jen.sagepub.com
SAGE

# Temperature and moisture storage in crop-based materials: Modelling a straw bale wall subject to a thermal shock

**Dubois Samuel[1], Evrard Arnaud[2], Blecker Christophe[1] and Lebeau Frédéric[1]**

**Abstract**

Modelling the hygrothermal behaviour of crop-based insulation products is essential to assess their impact on the energy performance of the building, predict indoor climate conditions, and prevent any risk of unexpected degradation. Traditionally, transient numerical models that predict internal conditions of construction materials consider that the variation of moisture storage with temperature is negligible although the sorption behaviour is known to be temperature dependent. This paper investigates this particular effect for crop-based materials and uses a refinement of standard mathematical representations. For this purpose, the effects of a thermal shock on the evolution of hygrothermal conditions inside a straw-bale wall are studied with several versions of a flexible research model. The latter is capable of incorporating the temperature dependency of the sorption curve with both a physically-based and an empirical description. A large climate chamber is used to gather experimental data and is able to host a full-size straw bale prefabricated panel. Internal conditions of straw bales are obtained with proper sensors bars. Results show that when large temperature gradients occur in a crop-based material, a model that considers temperature effect on moisture storage enhances greatly the prediction of internal conditions.

[1]Gembloux Agro-Bio Tech, Université de Liège, Gembloux, Belgium

[2]Architecture et Climat, Université Catholique de Louvain, Louvain-la-Neuve, Belgium

**Corresponding author:**
Dubois Samuel, Gembloux Agro-Bio Tech, Université de Liège, Passage des Déportés 2, 5030 Gembloux, Belgium.
Email: sdu@bbri.be

**Keyword**
HAM modelling, Bio-based materials, Hygroscopicity, Thermal shock, Straw bale

## Introduction

Straw bales have been successfully used as building material in the last century, either in load-bearing or infill techniques (King, 2006). Interest in this atypical product has recently resurfaced mainly due to sustainability and health-related qualities (Cripps et al., 2004) associated with good thermal and acoustic performance (Fuchs et al., 2009; Shea et al., 2013). Moreover, such crop-based materials are characterized by their moisture storage and exchange capacity, which may have a direct impact in terms of comfort and energy consumption (Madurwar et al., 2013; Osanyintola and Simonson, 2006). The extent of these phenomena is related to the porous structure of the material as the latter will determine the sorption and capillary properties as well as heat and moisture transfer functions. An accurate prediction of the underlying physical phenomena is thus critical to assess the specific advantages arising there from.

Heat, air and moisture (HAM) models were developed in order to predict coupled heat and mass transfers in porous media. The use of non-linear partial differential equations (PDEs) with numerical solvers is the more accurate technique to account for the complexity of highly hygroscopic products' behaviour. Many available models are able to perform such computations and were compared in previous studies (Delgado et al., 2013; Hagentoft et al., 2004; Janssens et al., 2008). From the mathematical point of view, they differ mainly in the underlying assumptions and resulting simplifications in the mathematical expressions. Additionally, some authors (Tariku et al., 2010; Van Schijndel, 2009) showed that models developed in general computational software are attractive in terms of evolution potential and interoperability with other computational tools. Recently, Dubois et al. (2013) illustrated how a heat and moisture transfer model developed in the COMSOL Multiphysics software can be used to accurately simulate highly hygroscopic materials during a moisture buffer value evaluation test. Now, this numerical tool can be further validated by confrontation to case studies where materials are subject to strongly non-isothermal conditions. In fact, there are still very few validation studies in which hygroscopic materials are subject to significant temperature gradients in literature related to HAM models.

One of the most frequent hypotheses in HAM models is to neglect the effect of temperature on moisture storage (Hens, 2008). Most of them use a unique moisture storage curve (MSC) to express the relationship between equilibrium moisture content (EMC) and relative humidity (RH) in hygroscopic materials, a function needed to solve the moisture balance equation. Exhaustive studies related to moisture storage in wood and plant fibres can be found (Simpson, 1980; Strømdahl, 2000; Time, 1998) and it is now widely accepted that the

variation of EMC with temperature exists in the hygroscopic domain and is linked to the thermodynamics of sorption. Hereafter, we aim to benefit from the modularity of the proposed heat and moisture transfer to test different moisture storage descriptions in parallel and evaluate their efficiency when applied to crop-based products modelling.

In this article, the modelling of a straw bales panel subjected to a thermal shock is investigated. The first part of the study describes the experimental set-up involving a large scale climate chamber and specific sensors that are used to produce the validation data. In a second step, a research model is presented along with different methods for characterizing the sorption curve dependence on temperature. Among these techniques, an original method that relies on a single parameter definition is proposed. Finally, the experimental results are compared to the simulations of different versions of the model, one for each technique described and a version without temperature effect on moisture storage.

## Materials and methods

### *Test wall and hygrothermal sensors*

The tested straw bale panel assembly was produced by the Belgian company *Paille-Tech* (Evrard et al., 2012). Straw bales are used as infill in a wood-frame made of

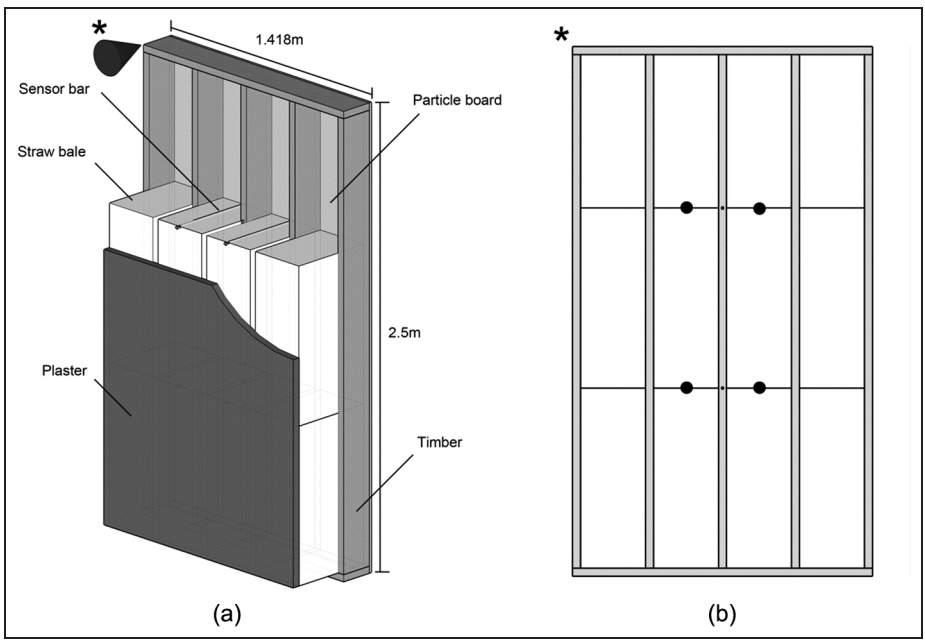


**Figure 1.** (a) Straw bales panel assembly and (b) sensor bars' location.

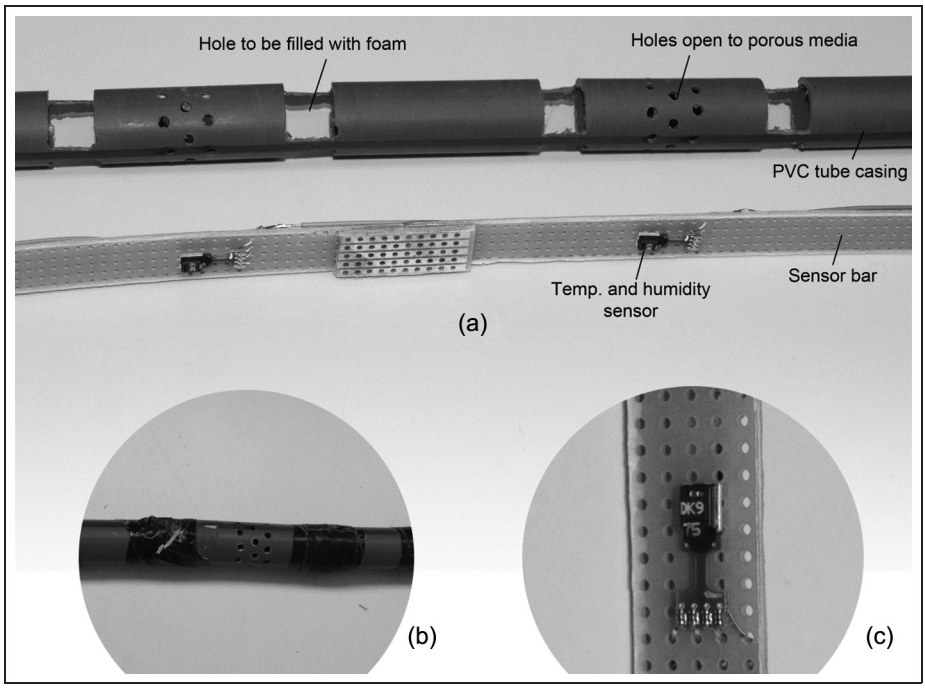


**Figure 2.** (a) Sensor bar description, (b) final aspect before insertion into the wall and (c) close-up of temperature and relative humidity sensor.

45-mm × 175-mm lumbers. Vertical studs are spaced at 345 mm on centre with bales stacked vertically between them. The resulting preferential orientation of straws is parallel to wall depth. To complete the structure, the frame is braced on the external side with breathable wood particle boards. On the internal side, the straw bales are covered with a 40-mm earth plaster. The details of construction are shown in Figure 1(a).

A common issue in measuring hygrothermal conditions inside high thickness materials is the assessment of the exact sensors' locations along the wall depth. Individual sensors are generally chosen for straw bales monitoring (Carfrae et al., 2009; Jolly, 2002), which requires a particular attention during assembly and does not provide a guarantee of equal sensor interspacing. In order to limit this source of error, rigid sensor bars were created instead, made from several sensing elements fixed on a rigid support. Each bar is composed of four SHT75 (*Sensirion*) digital temperature and RH sensors welded on a support board (Figure 2(c)). Each sensor is factory-calibrated and offers an accuracy of 1.8%RH on RH and 0.3 °C on temperature measurements in the typical ranges met in building materials. First, the sensors were welded on a Bakelite strip board with conductive copper bands (Figure 2(c)). This long plate was then protected in a polyvinyl chloride (PVC) tube of 15-mm diameter (Figure 2(a)). Perforations at the location of the sensors enable

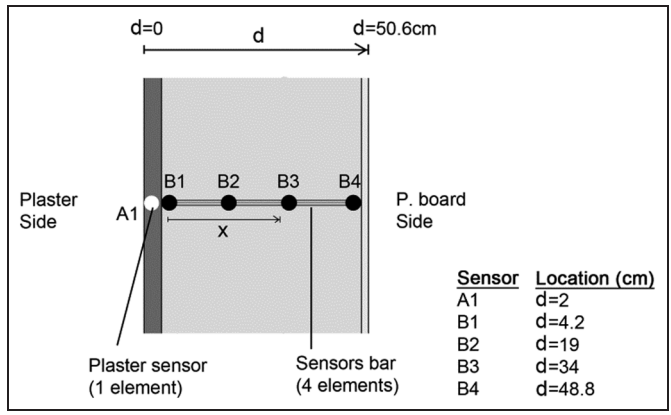


**Figure 3.** Final location of individual sensors.

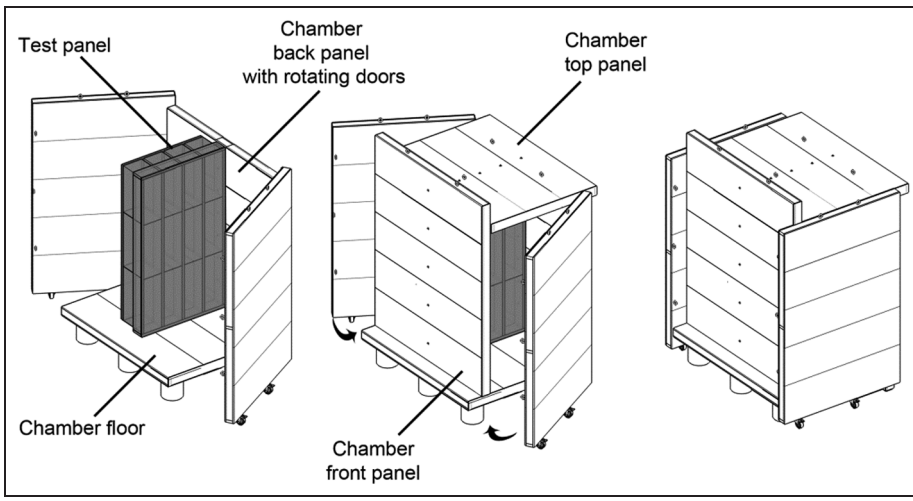


**Figure 4.** Modular climate chamber design.

the measurement. Finally, thermal insulation foam was injected between sensors through large holes provided for this purpose and protected with plastic tape (Figure 2(b)).

Four sensor bars were used to gather hygrothermal conditions in the straw bales along the wall depth (Figure 1(b)). In complement, individual SHT75 elements were incorporated in the plaster in the alignments of sensor bars. They are protected with a small concrete rawlplug. Figure 3 shows typical sensors alignment with resulting measurement points relative to wall depth.

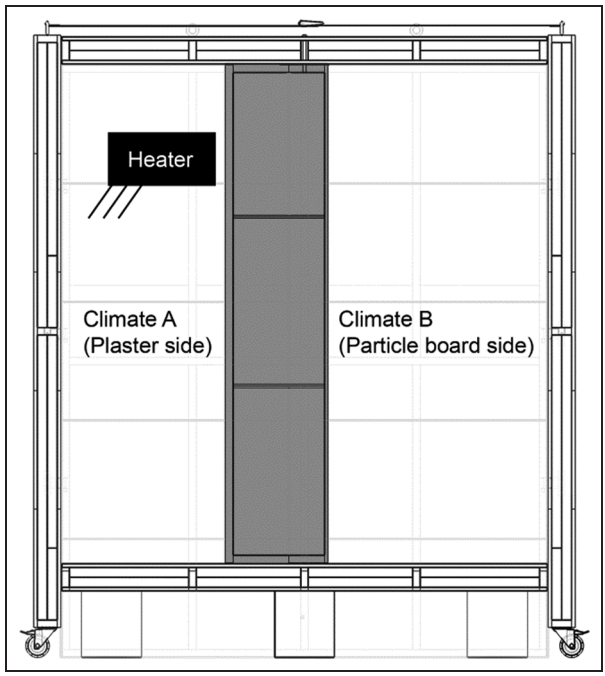


**Figure 5.** Bi-climatic system with heater on plaster side.

## *Thermal shock in a controlled climate chamber*

Various sizes of walls were planned to be tested with the device; therefore, the climatic chamber was made modular with a fixed base and some movable parts. A diagram illustrating the operation of a test wall is shown in Figure 4. The position of the floor and front chamber panels can be adjusted to fit the desired dimensions. Each structural panel composing the chamber is made from 100-mm × 38-mm timbers wood-frame closed with 18-mm oriented strand board (OSB) bracing. Extruded polystyrene provides thermal insulation and the inside surface is covered with a moisture barrier layer to avoid moisture movement from the inside air volume. The chamber panels were firmly fixed around the test wall with multiple bolts and compressible air tight joints on contact area.

Once the back panel rotating doors are closed, two climates can be controlled and monitored on each side of the test wall. That is why the testing device can be referred to as a 'Bi-climatic chamber' (Figure 5). It offers opportunities for 1D analysis of the wall assembly and was designed to impose various climatic schemes: realistic conditions or more artificial solicitations among which are hydric or thermal shocks. Here, a 2-kW pulsed air heater was placed in the 'Climate A' volume together with a proportional–integral–derivative (PID) control system. At the beginning of the experiment, a temperature step was applied on the plaster side of

the wall (from room temperature ≈20 °C to 35 °C). After 54 h, the heating system was switched off and the two doors of the climate chambers were opened to the hall climate. The entire monitoring system continues to log data for another 20 days. During the entire test, Climate B was not controlled. In addition to panel sensors, four Temperature/RH sensors were placed in each sub-chamber at various height levels to get an averaged measurement of climates A and B hygrothermal conditions. The sampling rate of every sensor is one measurement per minute. It should be known that the entire test chamber itself lies in a workshop hall where temperature and humidity fluctuations are low.

## Hygrothermal model

*General assumptions and macroscopic balance equations.* A combined heat and moisture transfer model was previously developed in COMSOL Multiphysics to simulate a case study in which temperature gradients are expected to be low (Dubois et al., 2013, 2014). The model was upgraded here to confront the thermal shock study by incorporating a temperature dependence of moisture content.

The simulated straw bales are considered as a 1D multiphase system and the developed conservation PDEs are based on volume averaging theory (Whitaker, 1977). For the present research, the balance equation system was solved for RH and temperature as main dependent variables. Equation (1) shows the moisture mass conservation equation

$$\rho_0 \xi_\varphi \frac{\partial \varphi}{\partial t} + \rho_0 \xi_T \frac{\partial T}{\partial t} = -\frac{\partial}{\partial x}\left[\underbrace{-\frac{\delta_{air}\varphi}{\mu}\frac{\partial p_{sat}}{\partial T}\frac{\partial T}{\partial x} - \frac{\delta_{air} p_{sat}}{\mu}\frac{\partial \varphi}{\partial x}}_{j_x^{M_v}}\right] \tag{1}$$

where $\boldsymbol{j}_{\boldsymbol{x}}^{\boldsymbol{M_v}}(\mathrm{kg}\cdot\mathrm{m}^{-2}\cdot\mathrm{s}^{-1})$ is the vapour diffusion flux density, $\rho_0(\mathrm{kg}\cdot\mathrm{m}^3)$ is the bulk density of the material, $u(\mathrm{kg}\cdot\mathrm{kg}^{-1})$ is the material moisture content, $\delta_{air}(\mathrm{kg}\cdot\mathrm{m}^{-1}\cdot\mathrm{s}^{-1}\cdot\mathrm{Pa}^{-1})$ is the vapour permeability of dry air and $\mu(-)$ is the vapour resistance factor of the material, considered constant during the thermal shock. This parameter does not strictly account for vapour transport but also handles other moisture transport modes occurring in the hygroscopic moisture content range, namely capillary water transport in very small pores and multilayered adsorbed water diffusion. The hypothesis of a constant value only holds if RH variation is moderate. On the left hand side, the moisture capacity terms $\xi_\varphi(\mathrm{kg}\cdot\mathrm{kg}^{-1})$ and $\xi_T(\mathrm{kg}\cdot\mathrm{kg}^{-1}\cdot\mathrm{K}^{-1})$ represent the variation of moisture content with RH at constant temperature $\partial u/\partial\varphi|_T$ and the variation of moisture content with temperature at constant RH $\partial u/\partial T|_\varphi$, respectively. The second term only exists if temperature is assumed to influence moisture storage. On the right hand side of the equation, it is observed that neither liquid transfer nor advective vapour fluxes are

accounted for as they are assumed to play only a little role during the simulated heat shock.

Applying the law of conservation of heat, the enthalpy change in an averaged volume element is determined by the divergence of heat conduction flux density, by sensible heat transport and by latent heat involved in the phase change process

$$\frac{\partial H}{\partial t} = \frac{\partial}{\partial x}\underbrace{\left[\lambda_{eff}\frac{\partial T}{\partial x}\right]}_{Conduction} - \underbrace{j_x^{M_v}\cdot c_v\frac{\partial T}{\partial x}}_{Sensible\ heat} - \underbrace{\dot{m}(Q_{st})}_{latent\ heat} \tag{2}$$

where $H(\mathrm{J}\cdot\mathrm{m}^{-3})$ is the enthalpy, $\dot{m}(\mathrm{kg}\cdot\mathrm{m}^{-3}\cdot\mathrm{s}^{-1})$ is the phase change rate, $\lambda_{eff}$ is the effective thermal conductivity of the material and $Q_{st}(\mathrm{J}\cdot\mathrm{kg}^{-1})$ is the amount of energy involved in the sorption process, known as the isosteric heat of sorption. Under the assumption that moisture storage in vapour phase is negligible compared to liquid phase, the phase change rate term is equal to the vapour flux divergence. The effective thermal conductivity is considered constant during the thermal shock, and its value was chosen to account for an average value met during the thermal shock. By developing the enthalpy term, the heat balance equation becomes

$$\frac{\partial(\rho_0 c_0(T-T_0)+\rho_0 u c_l(T-T_0))}{\partial t} = \frac{\partial}{\partial x}\left[\lambda_{eff}\frac{\partial T}{\partial x}\right] - j_x^{M_v}\cdot c_v\frac{\partial T}{\partial x} - \frac{\partial j_x^{M_v}}{\partial x}\cdot(Q_{st}) \tag{3}$$

Finally, with additional transformations and the assumption that sensible heat transport is negligible in comparison to latent heat, the heat balance equation becomes

$$\rho_0(c_0 + u c_l + \xi_T c_l(T-T_0))\frac{\partial T}{\partial t} + \rho_0\xi_\varphi\frac{\partial \varphi}{\partial t}c_l(T-T_0) = \frac{\partial}{\partial x}\left[\lambda_{eff}\frac{\partial T}{\partial x}\right] - \frac{\partial j_x^{M_v}}{\partial x}(Q_{st}) \tag{4}$$

*Temperature effect on moisture storage.* When water molecules are absorbed on the inner porous structure, some heat of sorption is released, and a corresponding amount of energy is required to desorb it. This enthalpy change is greater than the heat of vapourization of free water $L(\mathrm{J}\cdot\mathrm{kg}^{-1})$, and the difference is expressed as the differential heat of sorption or net isosteric heat $q_{st}(\mathrm{J}\cdot\mathrm{kg}^{-1}) = Q_{st} - L$. This quantity depends on the moisture content because successive water molecule layers show different bonding energy to the solid matrix of the material. One of the methods to determine this function is based on the Clausius–Clapeyron (CC) formula (Skaar, 1972). With a minimum of two sorption curves data sets, measured at different temperatures, we have

$$q_{st}(u) = R_v \ln\left(\frac{\varphi_{T1}(u)}{\varphi_{T2}(u)}\right)\left(\frac{T_1 T_2}{T_1 - T_2}\right) \tag{5}$$

where $R_v(\mathrm{J}\cdot\mathrm{kg}^{-1}\cdot\mathrm{K}^{-1})$ is the water vapour specific gas constant and $\varphi_{T1}(u)$ and $\varphi_{T2}(u)$ are the sorption isotherms at temperatures $T_1$ and $T_2$, respectively. From this

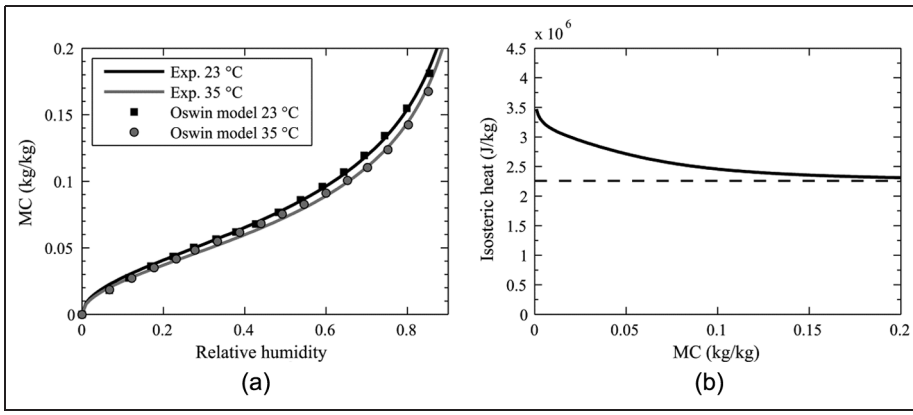


**Figure 6.** (a) Measured sorption isotherms of straw at 23 °C and 35 °C fitted with Oswin model and (b) net isosteric heat.

equation, it is easily observed that the EMC increases with decreasing temperature with a maximum at 0 °C (Cudinov and Andreev, 1978).

Sorption curves of straw bales were measured on the 0%RH–90%RH range at 23 °C and 35 °C with a dynamic vapour sorption (DVS) apparatus. This device was precisely parameterized to account for the specific equilibrium time observed for the straw material for each temperature. The Oswin moisture storage function (Oswin, 1946) was then fitted on resulting ($\varphi_i$, $u_i$) experimental points. It offers a continuous expression of moisture content in dependence with RH

$$u(\varphi) = C \times \left(\frac{\varphi}{1-\varphi}\right)^n \tag{6}$$

where $C$ and $n$ are constant parameters, estimated independently for the two temperatures by minimizing the sum of squared residuals. Best parameters are $C = 0.0793$ and $n = 0.48$ to fit the sorption isotherm at 23 °C and $C = 0.0730$ and $n = 0.49$ for sorption isotherm at 35 °C. Figure 6(a) shows the two measured sorption isotherms together with the fitted Oswin storage functions, and Figure 6(b) shows the net isosteric heat computed for straw using equation (5).

Once the net isosteric heat function is known or determined on the basis of two sorption isotherms, Poyet and Charles (2009) showed that the CC equation can be arranged to construct a temperature-dependent expression of the moisture storage by expressing the equilibrium RH as

$$\varphi(u,T) = \varphi_{Tref}(u) \cdot \exp\left[\frac{q_{st}(u)}{R_v}\left(\frac{T-T_{ref}}{TT_{ref}}\right)\right] \tag{7}$$

where $\varphi_{Tref}(u)$ is a reference sorption curve at temperature $T_{ref}$, which in our study can be either 23 °C or 35 °C. One of the big advantages of this method is that any

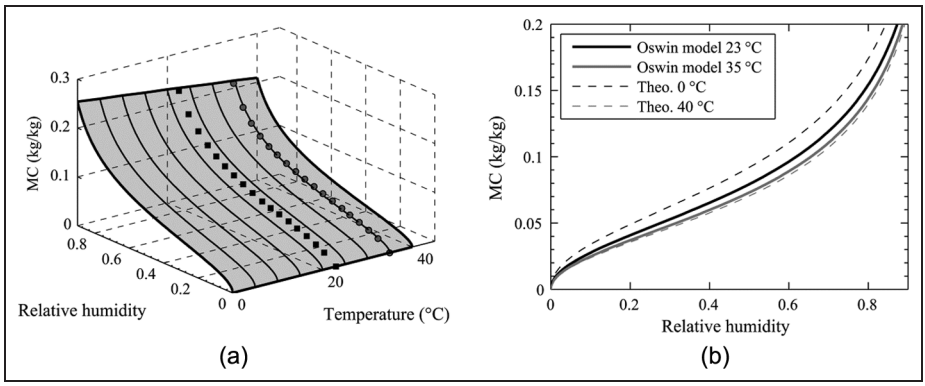


**Figure 7.** (a) Temperature-dependent MSC constructed by linearization between nine isotherms and (b) theoretical MSCs of straw at 0 °C and 40 °C with physically based model and the two experimental curves used to determine them.
MSC: moisture storage curve.

model can be used to describe this reference isotherm. However, in order to solve the heat shock case study, a continuous expression in the form $u(\varphi, T)$ is desirable. Indeed, such 'three-dimensional (3D)' representation of the moisture content $u$ would provide values for moisture capacities in all combinations of temperature and humidity conditions that are potentially met in the material. Unfortunately, equation (7) is not directly reversible and two different approaches were undertaken to overcome this issue. These approaches result in two different descriptions of the moisture storage function $u(\varphi, T)$, one is physically based and the other is purely empirical.

The most physically accurate method is to create an arbitrary number of MSCs $\varphi(u, T_i)$ at different temperatures $T_i$ using equation (7). Then, it is possible to obtain the continuous $u(\varphi, T)$ expression by linear interpolation between the reciprocal of these individual isotherms. This operation requires that 3D interpolation is available in the numerical environment.

An interpolated 'surface', based on nine individual curves, is shown in Figure 7(a). As an illustration purpose, the two boundary isotherms, which correspond to 0 °C and 40 °C, are shown in Figure 7(b). We recall that only the adsorption curve is considered in this work as hysteresis phenomena are assumed to be negligible in the heat shock working range.

The second modelling technique studied here is characterized by a simpler representation of temperature effect on moisture storage. In contrast to the physically based method embodied in equation (7), Keey (1978) proposed an empirical expression of thermal moisture capacity assuming a linear dependence on moisture content

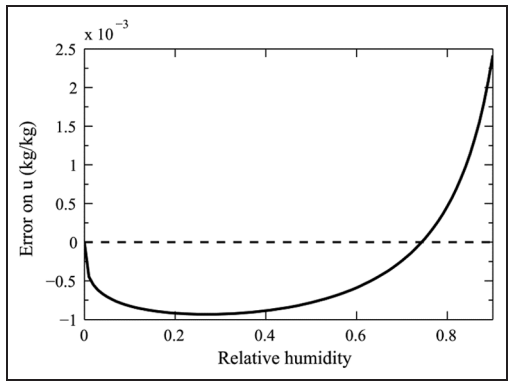


**Figure 8.** Error of the second method to obtain the temperature-dependent MSC, for $A = 0.0058$.
MSC: moisture storage curve.

$$\left.\frac{\partial u}{\partial T}\right|_{\varphi} = -A \cdot u \tag{8}$$

According to Keey, the parameter $A(\mathrm{K}^{-1})$ lies between 0.005 and 0.01 for wood, for RH values in the 10%RH–90%RH range. On the basis of this simplified assumption, we propose to write the following expression for the temperature-dependent MSC

$$u(\varphi, T) = u_{Tref}(\varphi) \cdot \left(1 - A\left(T - T_{ref}\right)\right) \tag{9}$$

where $u_{Tref}(\varphi)$ is the Oswin storage function whose parameters are fitted on experimental points measured at temperature $T_{ref}$. Here, the 23 °C experimental sorption isotherm is chosen arbitrarily as reference. The value of parameter $A$ was optimized to minimize the difference between the computed curve and experimental measurements for a temperature of 35 °C. This optimization led to a value of $A = 0.0058$ with a residual error given in Figure 8.

## Modelling procedure

*Model versions.* The chosen computing environment provides direct access to mathematical expressions, which allows high modularity depending on the case study and potential efficiency enhancement. Three different versions of the COMSOL model were prepared in order to analyse the impact of the moisture storage description on output error, given the results from the thermal shock experiment. Table 1 provides the balance equations and moisture content description for all three versions.

Version 1 represents the most complex description; the MSC is constructed on the basis of the physically based description of EMC dependence on temperature

**Table 1.** The three versions of the model.

| Version 1 – Temperature effect on MSC: physically based | |
|---|---|
| Balance equations | Moisture storage |
| $\rho_0 \xi_\varphi \frac{\partial \varphi}{\partial t} + \rho_0 \xi_T \frac{\partial T}{\partial t} = -\frac{\partial}{\partial x}\left[-j_x^{M_v}\right]$<br>$\rho_0 (c_0 + u c_l + \xi_T c_l (T - T_0)) \frac{\partial T}{\partial t}$<br>$+ \rho_0 \xi_\varphi \frac{\partial \varphi}{\partial t} c_l (T - T_0) = \frac{\partial}{\partial x}\left[\lambda_{eff} \frac{\partial T}{\partial x}\right] - \frac{\partial j_x^{M_v}}{\partial x}(L + q_{st}(u))$ | $u(\varphi, T)$ interpolated from nine isotherms individually computed from<br>$\varphi(u, T_i) = \varphi_{Tref}(u)$<br>$\cdot \exp\left[\frac{q_{st}(u)}{R_v}\left(\frac{T_i - T_{ref}}{T_i T_{ref}}\right)\right]$ |
| **Version 2 – Temperature effect on MSC: one-parameter empirical description** | |
| Balance equations | Moisture storage |
| $\rho_0 \xi_\varphi \frac{\partial \varphi}{\partial t} + \rho_0 \xi_T \frac{\partial T}{\partial t} = -\frac{\partial}{\partial x}\left[-j_x^{M_v}\right]$<br>$\rho_0 (c_0 + u c_l + \xi_T c_l (T - T_0)) \frac{\partial T}{\partial t}$<br>$+ \rho_0 \xi_\varphi \frac{\partial \varphi}{\partial t} c_l (T - T_0) = \frac{\partial}{\partial x}\left[\lambda_{eff} \frac{\partial T}{\partial x}\right] - \frac{\partial j_x^{M_v}}{\partial x}(L)$ | $u(\varphi, T) = u_{Tref}(\varphi)$<br>$\cdot \left(1 - A\left(T - T_{ref}\right)\right)$ |
| **Version 3 – Temperature effect on MSC: none** | |
| Balance equations | Moisture storage |
| $\rho_0 \xi_\varphi \frac{\partial \varphi}{\partial t} = -\frac{\partial}{\partial x}\left[-j_x^{M_v}\right]$<br>$\rho_0 (c_0 + u c_l) \frac{\partial T}{\partial t} + \rho_0 \xi_\varphi \frac{\partial \varphi}{\partial t} c_l (T - T_0)$<br>$= \frac{\partial}{\partial x}\left[\lambda_{eff} \frac{\partial T}{\partial x}\right] - \frac{\partial j_x^{M_v}}{\partial x}(L)$ | $u(\varphi) = C \times \left(\frac{\varphi}{1-\varphi}\right)^n$ |

MSC: moisture storage curve.

(equation (7)). It results that the net isosteric heat function is also included in the heat balance. In version 2, the model is simplified with the one-parameter description of moisture storage dependence on temperature (equation (9)). The isosteric heat is equal to the heat of vapourization of free water because no direct characterization of the differential heat of sorption can be obtained from this approach.

**Table 2.** Straw bales parameters used in simulations.

| Parameter | Unit | Value | Method |
|---|---|---|---|
| $\rho_0$ | $(kg \cdot m^{-3})$ | 100 | Estimated from standard values |
| $c_0$ | $(J \cdot kg^{-1} \cdot K^{-1})$ | 2426 | DTA |
| $\lambda_{eff}$ | $(W \cdot m^{-1} \cdot K^{-1})$ | 0.08 | Estimated from dry value (GHP) |
| $C_{23\,°C}$ | $(-)$ | 0.0793 | DVS |
| $n_{23\,°C}$ | $(-)$ | 0.48 | DVS |
| $C_{35\,°C}$ | $(-)$ | 0.0730 | DVS |
| $n_{35\,°C}$ | $(-)$ | 0.49 | DVS |
| $A$ | $(K^{-1})$ | 0.0058 | Estimated from DVS |
| $\mu$ | $(-)$ | 2 | Estimated from literature |

DTA: differential thermal analysis; GHP: guarded hot plate; DVS: dynamic vapour sorption.

Finally, version 3 is characterized by the standard description found in most HAM software packages, which is a single sorption isotherm. Similar to the version 2, the heat of sorption shows a simplified representation. It should be noted that all versions are similar with regard to the description of heat and moisture transport.

*Boundary and initial conditions.* In order to reduce the number of parameters needed to solve the problem, it was decided to limit the study domain to the straw bale material. The behaviours of the particle board and the plaster are not simulated. Dirichlet boundary conditions are thus applied to both extremities of the domain with temperature and RH values measured just behind the plaster (sensor B1) and just behind the particle board (sensor B4). Referring to Figure 3, we can write the following expressions for boundary and initial conditions

$$\begin{cases} \varphi(t) = \varphi_{B1}(t) \\ T(t) = T_{B1}(t) \end{cases} \quad x = 0\,\text{m} \quad (B1) \tag{10}$$

$$\begin{cases} \varphi(t) = \varphi_{B4}(t) \\ T(t) = T_{B4}(t) \end{cases} \quad x = 0.45\,\text{m} \quad (B4) \tag{11}$$

$$\begin{cases} \varphi(x,0) = \varphi_0(x) \\ T(x,0) = T_0(x) \end{cases} \quad 0 < x < 0.45\,\text{m} \tag{12}$$

where $\varphi_\alpha(t)$ and $T_\alpha(t)$ are the actual RH and temperature time series measured at sensor $\alpha$, respectively; $\varphi_0(x)$ is the initial RH vector and $T_0(x)$ is the initial temperature vector. The last two vectors are determined from initial temperature and RH measured at sensors B1, B2, B3 and B4.

*Straw bales properties.* For version 1 of the model, a total of eight material parameter values $(\rho_0, c_0, \lambda_{eff}, C_{T1}, n_{T1}, C_{T2}, n_{T1}, \mu)$ are needed in order to solve the heat and moisture balance equations (equations (1) and (4)) in the straw bale material, knowing the conditions imposed on its limits with B1 and B4 sensors. In order to solve version 2 of the model, the value of parameter $A$ is needed instead of two

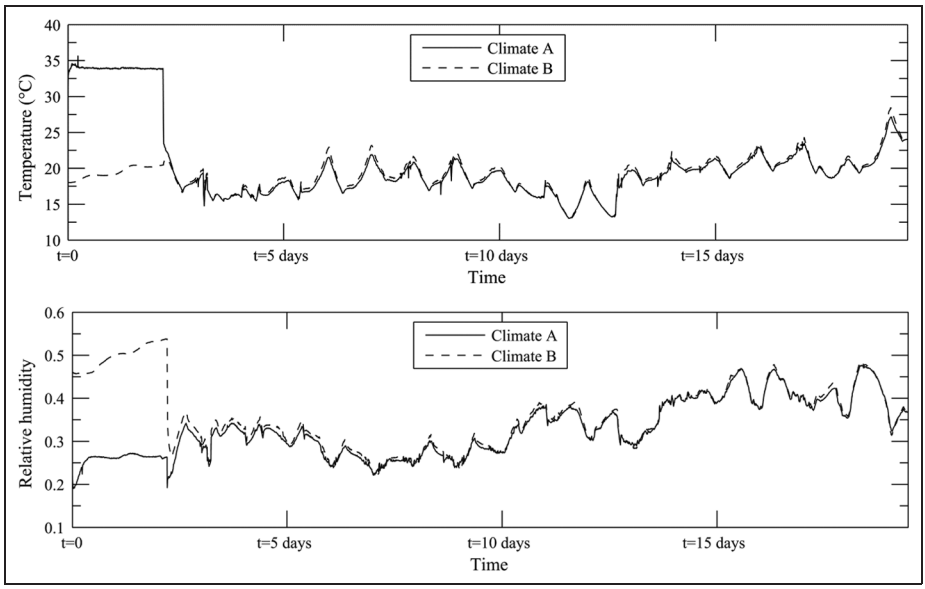


**Figure 9.** Temperature and relative humidity measured in sub-chambers A and B.

Oswin parameters needed in version 1 to define a second isotherm. Finally, the third version requires neither the definition of a second isotherm nor the value of parameter $A$.

Measuring all those parameters can be particularly tricky because of the size of straw bales and the intrinsic variability they show. The parameters used during the direct modelling approach are given in Table 2.

First, the bulk density is expected to be around the 80–120 kg $m^{-3}$ range, but it is impossible to know the actual value for the straw bales incorporated in the panel. In consequence, the median value was implemented in simulations. The dry thermal capacity was determined by differential thermal analysis on a crushed sample previously dried. A guarded hot plate (GHP) apparatus designed for high thickness specimens (Dubois and Lebeau, 2013) was used to determine the dry thermal conductivity of an entire straw bale at 20 °C. With thermal flow parallel to fibres, the value obtained was $\lambda_0 = 0.0682\,\mathrm{W \cdot m^{-1} \cdot K^{-1}}$. In subsequent simulations, a constant effective thermal conductivity is used, $\lambda_{eff}$, which represents an averaged value over conditions met during the test. In consequence, it should be expect to be higher than the measured conductivity.

In section 'Temperature effect on moisture storage', the values for the Oswin model parameters were presented, on the basis of DVS measurement analysis. It was also described how the value of parameter $A$ could be obtained. With one or the other technique retained for the description of the temperature effect on moisture storage, the isothermal and non-isothermal moisture capacity functions $\xi_\varphi(\varphi, T)$ and $\xi_T(\varphi, T)$ are then easily determined. A large uncertainty remains

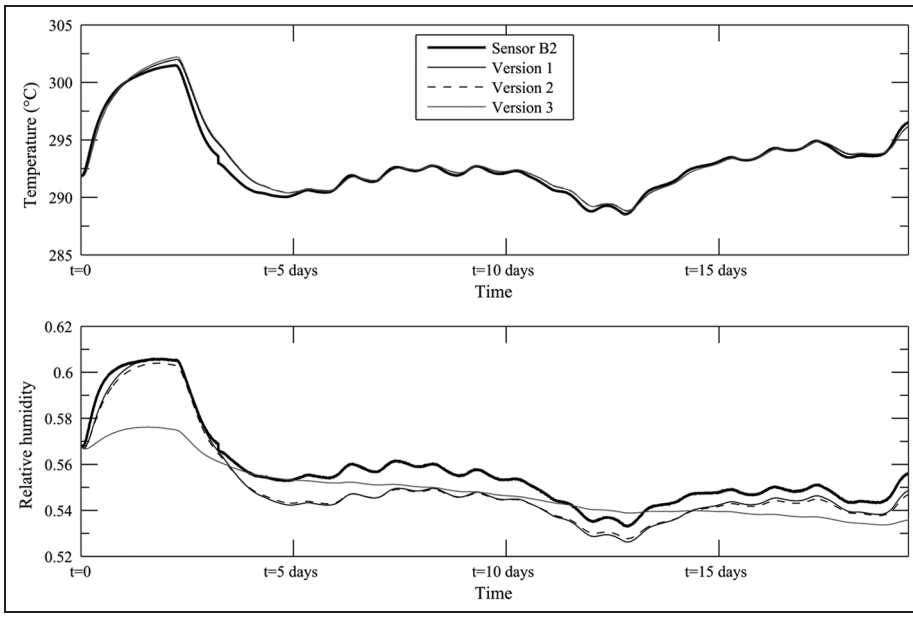


**Figure 10.** Simulation results for the three model versions compared to experimental data (sensor B2).

concerning the actual moisture content modification with temperature and the 'representativeness' of the chosen mathematical description which has to be confirmed in this research. Finally, the vapour resistance factor of straw is quite difficult to measure with standard dry- or wet-cup methods. At first approximation, its value was fixed based on the work of Wihan (2007). As for effective thermal conductivity, a constant vapour transport is assumed given the lack of available data in literature and the difficulties in assessing the vapour transport variation with dependent variables. However, it can be expected to be negligible based on measurements performed on other materials and expected conditions in the straw bales during the thermal shock (Galbraith et al., 2000).

## Results and discussions

### *Sub-chambers' sensor data*

The temperature measured in sub-chambers A and B is shown in Figure 9. The temperature is maintained around 34 °C in the A air volume during the first 54 h of the test. Then, as the doors of the chamber are opened on both end sides, its value drops rapidly to meet the hall temperature. Thereafter, the temperature measured in both sub-chambers corresponds to the variations occurring in the large test hall

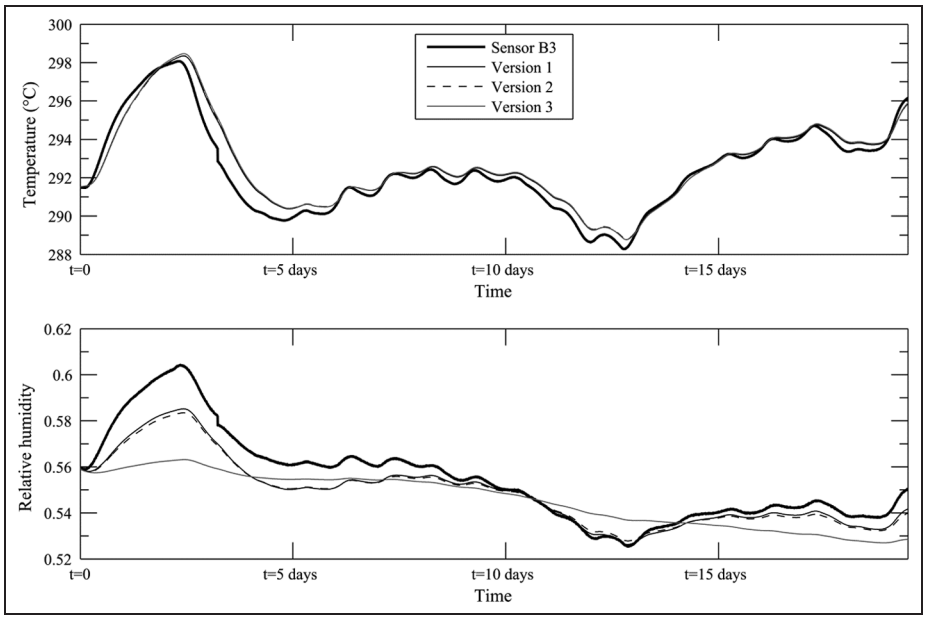


**Figure 11.** Simulation results for the three model versions compared to experimental data (sensor B3).

**Table 3.** Efficiency criteria computed for all model versions and temperature and relative humidity separately.

| | Temperature | | | Relative humidity | | |
|---|---|---|---|---|---|---|
| | NSE | PBIAS | RMSE | NSE | PBIAS | RMSE |
| Version 1 | 0.966 | −0.07% | 0.502 | 0.834 | 1.13% | 0.0077 |
| Version 2 | 0.962 | −0.08% | 0.530 | 0.819 | 1.19% | 0.0080 |
| Version 3 | 0.958 | −0.09% | 0.553 | 0.504 | 1.57% | 0.0133 |

NSE: Nash–Sutcliffe efficiency; PBIAS: percent bias; RMSE: root mean square error.

where the device was placed. Values oscillated around 20 °C following a natural daily cycle with higher temperature during the day.

## *Numerical results*

Figure 10 presents the temperature and RH simulated at B2 sensor location by the three versions of the model compared to measured data. Figure 11 provides the same information at B3 sensor location, a bit further in the straw depth relatively to the thermal shock progression. No distinction can be made visually between

models concerning the temperature field modelling. The output of all versions seems to compare quite well to experimental temperature in the case of sensor B2. A small delay can be observed between experimental and numerical temperature peaks for sensor B3. This could be explained most likely by small errors in the definition of the straw inertia through density and heat capacity parameters. Concerning the RH field, version 3 of the model clearly underscored in modelling performance. For both sensors, it seems that the version only accounts for the general humidity decreases which can be observed throughout the entire test period. All the higher frequencies of humidity variation, apparently linked to the temperature variation, are not modelled by this simplest description.

To enlarge the discussion, some efficiency criteria were computed for all simulations and are summarized in Table 3. We used the Nash–Sutcliffe efficiency (NSE) coefficient, the percent bias (PBIAS) and the root mean square error (RMSE) as defined in Dubois et al. (2013). Results are presented for temperature and RH data sets separately but both sensors' locations are considered together.

For temperature field modelling, all model versions show a similar efficiency with $NSE > 0.95$. The improvement of efficiency respects the simplification magnitude in the mathematical description as version 1 performs slightly better than version 2 that shows itself a better NSE and RMSE than version 3. They all show a little tendency to overestimate temperature as PBIAS is around $-0.1\%$. The internal RH modelling is clearly less accurate with the standard HAM description corresponding to version 3. The NSE rises spectacularly when the effect of a variable isotherm is included.

It is observed that the formulation proposed by Keey (equation (12)) and the corresponding proposal for continuous expression of MSC give a good representation of straw behaviour, which is only slightly improved by the physically based approach. This simple formulation offers advantages in terms of model coding and computational time. In specific application where temperature gradients are high, it offers a simple way to account for temperature dependence of moisture content. The temperature effect on moisture storage is then characterized with only one parameter, whereas the physically based method requires at least two parameters, that is, to characterize a second complete isotherm in order to define the net isosteric heat function.

In the previous sections, we showed that much uncertainty remains in the characterization of the straw bale material. First, a lot of simplification hypotheses were assumed during these simulations: absence of liquid transport, constant transport coefficients and no hysteresis phenomena. It seems clear that considering these different effects could improve further the efficiency, but it might require an unnecessary amount of efforts compared to the additional efficiency that results. When using constant material parameters, some large obstacles still remain in determining their values for such unusual construction product. In that context, inverse modelling techniques, as presented in Dubois et al. (2014), could offer an original way of improving simulations. The benefit of having one unique parameter for modelling the temperature effect on moisture storage would then be directly recoverable when

performing parameter optimization. The inverse modelling approaches also allow us to analyse experimental parameters. In the experiment presented here, the location of sensors is still subject to some uncertainty even if the 'sensor bar' offers a significant improvement in comparison to traditional single-point measurements.

## Conclusion

In this article, a flexible numerical model for heat and moisture transfer in building materials is used to simulate the behaviour of a hygroscopic wall assembly under non-isothermal solicitations. A prefabricated straw bale panel was first subjected to a 35 °C thermal shock in a climate chamber. Specific T/RH sensors were created to answer the need for proper sensing location. The monitoring of internal conditions in straw bales during this test constitutes the measurement data intended to be compared with the output of the model.

The numerical model used to describe the heat and moisture transfer in the straw during the heat shock is developed in COMSOL and uses a mass balance equation in which moisture content variation with temperature can be considered. Two approaches were chosen to characterize a continuous 'sorption surface' with RH and temperature dependency. The upgrading potential of the model is highlighted as three different versions are studied based on the type of moisture storage description.

This study shows that a one-parameter empirical approach to describe temperature effect on moisture storage can enhance greatly the efficiency of a HAM model in comparison to the frequent isothermal sorption characteristic assumption. This technique is easy to implement and offers a true continuous description of moisture capacities. The physically based method needs to be constructed from multiple individual isotherms and only offers a slight further improvement. It should be specified that these refinements might become insignificant when temperature gradients are moderate, as often in normal use conditions of a building. A better definition of material parameters should then provide a better source for prediction optimization. Still, this article proves that in some particular conditions, the single isotherm assumption does not transpose adequately the actual behaviour of crop-based materials. The one-parameter description of the temperature effect on moisture storage would then be a useful model improvement, allowing us to deepen the understanding of complex hygroscopic materials especially through the use of parameter optimization.

### Declaration of conflicting interests

The authors declared no potential conflicts of interest with respect to the research, authorship, and/or publication of this article.

## Funding

This work was supported by the *FNRS (Fonds National de la Recherche Scientifique)* in Belgium (FRIA grant).

## References

Carfrae J, De Wilde P, Littlewood J, et al. (2009) Long term evaluation of the performance of a straw bale house built in a temperate maritime climate. In: *11th international conference on non-conventional materials and technologies*, Bath, 6–9 September.

Cripps A, Handyside R, Dewar L, et al. (2004) *Crops in Construction Handbook* (Report). London: CIRIA.

Cudinov B and Andreev M (1978) Hygroscopicity of wood at temperatures below zero degrees centigrade. 2. The condition of the hygroscopic moisture and the equilibrium moisture content, Leipzig, VEB Fachbuchverlag. *Holztechnologie* 19: 147–151.

Delgado JM, Barreira E and Ramos NM (2013) *Hygrothermal Numerical Simulation Tools Applied to Building Physics*. Berlin: Springer.

Dubois S and Lebeau F (2013) Design, construction and validation of a guarded hot plate apparatus for thermal conductivity measurement of high thickness crop-based specimens. *Materials and Structures*. Epub ahead of print 18 October. DOI: 10.1617/s11527-013-0192-4.

Dubois S, Evrard A and Lebeau F (2013) Modeling the hygrothermal behavior of biobased construction materials. *Journal of Building Physics*. Epub ahead of print 14 June. DOI: 10.1177/1744259113489810.

Dubois S, McGregor F, Lebeau F, et al. (2014) An inverse modelling approach to estimate the hygric parameters of clay-based masonry during a moisture buffer value test. *Building and Environment* 81: 192–203.

Evrard A, Louis A, Biot B, et al. (2012) Moisture equilibrium in straw bales walls. In: *28th passive and low energy architecture conference*, Lima, 7–9 November.

Fuchs S, Krumm O and Cauderay E (2009) *La construction en botte de paille* (Report). Genève: ATBA.

Galbraith G, Guo J and McLean R (2000) The effect of temperature on the moisture permeability of building materials. *Building Research and Information* 28: 245–259.

Hagentoft C-E, Kalagasidis AS, Adl-Zarrabi B, et al. (2004) Assessment method of numerical prediction models for combined heat, air and moisture transfer in building components: benchmarks for one-dimensional cases. *Journal of Thermal Envelope and Building Science* 27: 327–352.

Hens H (2008) *Building Physics – Heat, Air and Moisture: Fundamentals and Engineering Methods with Examples and Exercises*. New York: John Wiley & Sons.

Janssens A, Woloszyn M, Rode C, et al. (2008) From EMPD to CFD – overview of different approaches for Heat Air and Moisture modeling in IEA Annex 41. In: *IEA ECBCS Annex 41 closing seminar*, Copenhagen, 19 June.

Jolly R (2002) *Straw Bale Moisture Monitoring Report* (Report). Ottawa, ON, Canada: CMHC.

Keey RB (1978) *Introduction to Industrial Drying Operations*. Oxford: Pergamon Press.

King B (2006) *Design of Straw Bale Buildings*. San Rafael, CA: Green Building Press.

Madurwar MV, Ralegaonkar RV and Mandavgane SA (2013) Application of agro-waste for sustainable construction materials: a review. *Construction and Building Materials* 38: 872–878.

Osanyintola OF and Simonson CJ (2006) Moisture buffering capacity of hygroscopic building materials: experimental facilities and energy impact. *Energy and Buildings* 38: 1270–1282.

Oswin C (1946) The kinetics of package life. III. The isotherm. *Journal of the Society of Chemical Industry* 65: 419–421.

Poyet S and Charles S (2009) Temperature dependence of the sorption isotherms of cement-based materials: heat of sorption and Clausius–Clapeyron formula. *Cement and Concrete Research* 39: 1060–1067.

Shea A, Wall K and Walker P (2013) Evaluation of the thermal performance of an innovative prefabricated natural plant fibre building system. *Building Service Engineering Research and Technology* 34: 369–380.

Simpson W (1980) Sorption theories applied to wood. *Wood and Fiber Science* 12: 183–195.

Skaar C (1972) *Water in Wood*. Syracuse, NY: Syracuse University Press.

Strømdahl K (2000) *Water sorption in wood and plant fibres*. PhD Thesis, Technical University of Denmark, Kongens Lyngby.

Tariku F, Kumaran K and Fazio P (2010) Integrated analysis of whole building heat, air and moisture transfer. *International Journal of Heat and Mass Transfer* 53: 3111–3120.

Time B (1998) *Hygroscopic moisture transport in wood*. PhD Thesis, Norwegian University of Science and Technology, Trondheim.

Van Schijndel AWM (2009) Integrated modeling of dynamic heat, air and moisture processes in buildings and systems using SimuLink and COMSOL. *Building Simulation* 2: 143–155.

Whitaker S (1977) A theory of drying. *Advances in Heat Transfer* 13: 119–203.

Wihan J (2007) *Humidity in straw bale walls and its effect on the decomposition of straw*. PhD Thesis, School of Computing and Technology, University of East London, London.